

## Hall-coefficient factor and inverse valence-band parameters of holes in natural diamond

Lino Reggiani

*Gruppo Nazionale di Struttura della Materia, Istituto di Fisica dell'Università di Modena,  
via Campi 213/A, I-41100 Modena, Italy*

David Waechter and Stefan Zukotynski

*Department of Electrical Engineering and Centre for the Study of Materials,  
University of Toronto, Toronto, Ontario M5S 1A4, Canada*

(Received 18 August 1982; revised manuscript received 12 January 1983)

In strict analogy with the case of silicon, the Hall-coefficient factor of holes in natural diamond is found to be systematically less than unity in the range of temperature  $100 < T < 1000$  K investigated here. A microscopic interpretation is shown to provide information on the reliability of a different set of inverse valence-band parameters which can be found currently in the literature. Agreement between theory and experiment confirms the values  $|A| = 3.61$ ,  $|B| = 0.18$ , and  $|C| = 3.76$  deduced from pseudopotential band-structure calculations.

## I. INTRODUCTION

This paper reports on the dependence upon temperature of the Hall-coefficient factor  $r$ , phenomenologically defined as the ratio of the Hall and drift mobilities, i.e.,  $r = \mu_H / \mu_d$ , for the case of holes in natural diamond. The main objective of the paper is to obtain, from analysis of experimental data, information on the values of the inverse valence-band parameters for this material. At present, a number of different results for these parameters can be found in the literature. Our results render support to one of these sets.

Table I presents a summary of existing sets of band parameters in chronological order. For completeness, we also present the values of the density-of-states effective mass from (Ref. 1) and of the anisotropy factors, defined as the ratio between the heavy-hole wave vectors along given symmetry directions at the same energy under high-energy asymptotic conditions  $\epsilon / \Delta \gg 1$ . Subscripts  $h$ ,  $l$ , and  $so$  refer to heavy, light, and split-off band, respectively,  $\epsilon$  is the hole energy and  $\Delta = 0.006$  eV is the spin-orbit energy.

Band parameters I were obtained in pioneer band-structure calculations performed with the equivalent orbital method.<sup>2</sup> Set II was obtained from cyclotron resonance experiments.<sup>3</sup> Set III was obtained from a five-level  $\vec{k} \cdot \vec{p}$  analysis.<sup>4</sup> Sets IV, V, and VI are similar and were obtained from pseudopotential band-structure calculations.<sup>5-7</sup> In addition, the set V was shown to provide a satisfactory

interpretation of drift velocity experiments at high electric fields.<sup>8</sup>

In the high-energy range, i.e., for  $\epsilon \gg \Delta$ , the shape of equienergetic surface for sets IV, V, and VI displays a more pronounced anisotropic character (warped shape) than sets I, II, and III, as evidenced by the corresponding larger value of the anisotropy factor (see Table I). Since such an anisotropy of the hole equienergetic surfaces is known to strongly influence the Hall scattering factor by depressing its value with respect to an equivalent isotropic case,<sup>9,10</sup> the success of a band model in computing the Hall-coefficient factor is taken as indicative of its reliability.

Section II presents the theoretical model. Section III reports the available data for the Hall-coefficient factor and discusses the theoretical model.

## II. THEORY

The Hall-coefficient factor is calculated following the results of Ref. 9, thus, in what follows, only a brief description of the main features of the theory will be given.

As a starting point, we shall take the usual definition of the Hall-coefficient factor  $r$  for a single band appropriate to a cubic crystal:

$$r = n |q| \frac{\sigma_{123}}{(\sigma_{11})^2}, \quad (1)$$

where  $n$  is the carrier concentration,  $|q|$  the absolute value of the electron charge  $1.6 \times 10^{-19}$  C, and

TABLE I. Inverse valence-band parameters and related quantities in diamond.  $A$ ,  $B$ , and  $C$  are given in units of  $\hbar^2/2m$ , and the effective masses in terms of the free-electron mass,

$$\frac{k_{110}}{k_{100}} = \left[ \frac{2(1-b)}{2+b-3[(c^2/3)+b^2]^{1/2}} \right]^{1/2},$$

$$\frac{k_{111}}{k_{100}} = \left[ \frac{1-b}{1-[(c^2/3)+b^2]^{1/2}} \right]^{1/2},$$

where  $b = |B|/|A|$  and  $c = |C|/|A|$ .

	Band parameters					
	I Ref. 2	II Ref.3	III Ref. 4	IV Ref. 5	V Ref. 6	VI Ref. 7
$ A $	1.61	0.94	4.62	3.63	3.61	3.72
$ B $	0.11	0.44	0.84	0.44	0.18	0.42
$ C $	0.78	0.40	3.14	3.80	3.67	3.88
$m_h^a$	0.89	2.30	0.40	1.02	1.08	0.92
$m_1^a$	0.70	2.08	0.28	0.38	0.36	0.36
$m_{so}^a$	0.44	0.53	0.13	0.15	0.15	0.14
$k_{110}/k_{100}^a$	1.25	1.10	1.86	2.60	2.60	2.40
$k_{111}/k_{100}^a$	1.14	1.06	1.20	1.52	1.52	1.49

<sup>a</sup>Values are calculated under the asymptotic condition  $\epsilon/\Delta \gg 1$ .

$\sigma_{11}$  and  $\sigma_{123}$  are elements of the second rank conductivity tensor and of the third rank Hall-effect tensor, respectively. The coordinate axes are taken parallel to the crystal axes. In the relaxation-time approach,<sup>11</sup>

$$\sigma_{jl} = -\frac{q^2}{4\pi^3\hbar^2} \int \frac{\partial f_0}{\partial \epsilon} \tau(\epsilon) \frac{\partial \epsilon}{\partial k_j} \frac{\partial \epsilon}{\partial k_l} d^3k \quad (2)$$

and

$$\sigma_{jlm} = \frac{q^3}{4\pi^3\hbar^4} \int \frac{\partial f_0}{\partial \epsilon} \tau(\epsilon) \frac{\partial \epsilon}{\partial k_j} \times \left[ \frac{\partial \epsilon}{\partial k_r} \frac{\partial}{\partial k_s} \left( \tau(\epsilon) \frac{\partial \epsilon}{\partial k_l} \right) \right] \epsilon_{mrs} d^3k, \quad (3)$$

where  $\epsilon$  is the carrier energy,  $k$  the carrier wave vector,  $\tau$  the momentum relaxation time,  $f_0$  the Maxwell-Boltzmann equilibrium distribution function, and  $\epsilon_{mrs}$  the antisymmetric permutation tensor of Levi-Civita.

Generalization of  $r$  in Eq. (1) to the multiband system of the valence band leads to<sup>9</sup>

$$r = \frac{\sum_i n_i \sum_i n_i r_i \mu_{d,i}^2}{\left[ \sum_i n_i \mu_{d,i} \right]^2}, \quad (4)$$

where  $n_i$ ,  $r_i$ , and  $\mu_{d,i} = \sigma_{11}/(m_i |q|) = \sigma_{11}^{(i)}/(n_i |q|)$  are the concentration, the Hall-coefficient factor,

and the drift mobility of the individual valence bands, heavy, light, and split off, respectively.

The band model used accounts for heavy and light holes with the energy wave-vector dispersion relation obtained from the cubic equation reported in Kane's  $\vec{k} \cdot \vec{p}$  calculations.<sup>12</sup> The split-off band is ignored, by analogy with the case of Si,<sup>13,14</sup> in which it was found to be completely insignificant.

In the evaluation of the relaxation-time scattering by acoustic phonons, nonpolar optical phonons and ionized impurity scattering in the Brooks-Herring approach are considered. The analytical expression of the scattering rates is the same as in Ref. 15 where to simplify dealing with these scattering processes the following approximations were made.

For acoustic phonons, elastic scattering was assumed and the energy-equipartition approximation was used. In the range of temperatures here considered ( $T > 100$  K) both assumptions are well justified. Furthermore, a single coupling constant has been used rather than the original three deformation-potential parameters<sup>16,17</sup> and the effect of the overlap factor has been averaged and accounted for by the factor  $\frac{1}{2}$ .<sup>18</sup> In practice this approach, which is equivalent to neglecting effects associated with the anisotropy of the scattering, seems to be reasonable in view of the generally good results which have been obtained for the semiconductors Si and Ge.<sup>9</sup>

For ionized impurity scattering, interband scattering is rather small since the scattering probability

TABLE II. Constants of diamond, for references see Ref. 19.

Lattice constant	$a_0 = 3.57 \times 10^{-8}$ cm
Crystal density	$\rho = 3.51$ g cm $^{-3}$
Longitudinal sound velocity	$s_l = 18.21 \times 10^5$ cm sec $^{-1}$
Transverse sound velocity	$s_t = 12.30 \times 10^5$ cm sec $^{-1}$
Optical-phonon equivalent temperature	$\theta_{op} = 1938$ K
Static dielectric constant	$\epsilon_0 = 5.7$
Energy gap	$\epsilon_g = 5.49$ eV
Spin-orbit energy	$\Delta = 0.006$ eV
Acoustic deformation potential	$E_1^0 = 8.4$ (present work)
Optical deformation potential <sup>a</sup>	$(D_t K)_{op} = 3.4 \times 10^9$ eV cm $^{-1}$ (present work)
	$d_0 = 99.1$ eV

<sup>a</sup>The two formalisms are related by  $(D_t K)_{op} = (\frac{3}{2})^{1/2} d_0 / a_0$ .

decreases rapidly when the momentum change becomes larger, and therefore it has been neglected. Finally, in the evaluation of the scattering rate, the effect of warping has been averaged by integrating the  $\vec{k}$  dependence over the constant-energy surfaces.

### III. RESULTS AND DISCUSSION

Theoretical calculations of the Hall-coefficient factor have been performed by using the constants reported in Table II. Results obtained using the different sets of the valence-band parameters in Table I are reported as a function of temperature in Fig. 1 for the case when only lattice scattering is considered. It is worth noting that, within a few percent, these results have been found to be nearly independent of the values of the coupling constants; in any case, by scaling appropriately the deformation-potential parameters, different sets can be used to reproduce, within a comparable degree of accuracy, the temperature dependence of the drift mobility.

From Fig. 1 it is seen that the results can be gathered into two groups. This has been emphasized by the shaded regions in the figure. Accordingly, one group (i.e., sets I, II, and III) exhibits  $r$  values systematically greater than unity, while the second group (i.e., sets IV, V, and VI) exhibits values systematically lower than unity and very close to each other, so as to be not distinguishable in practice. In the same figure the experimental point at 300 K, which is taken as representative of data reported, strongly supports the validity of the latter group. When the value of  $m_h$  associated with each set of the latter group (see Table I) is considered, the better agreement with the value  $m_h = 1.1$  deduced from the saturation value of the high-field drift velocity<sup>19</sup> leads to set V being preferred over sets IV and VI. For this reason, in the discussion that follows only the calculations performed with set V will be reported.

Figures 2 and 3 enable us to analyze the Hall-coefficient factor, calculated with the set V, in terms of the different scattering contributions. From Fig. 2 it is seen that above about 500 K optical-phonon scattering tends to increase the value of  $r$  from its value associated with acoustic-phonon scattering. This result is similar to that obtained for the case of Ge.<sup>20</sup>

In Fig. 3 the effect of ionized impurity scattering upon the Hall-coefficient factor is analyzed by increasing impurity concentration up to  $N_I = 10^{16}$  cm $^{-3}$ . The effect becomes important below about

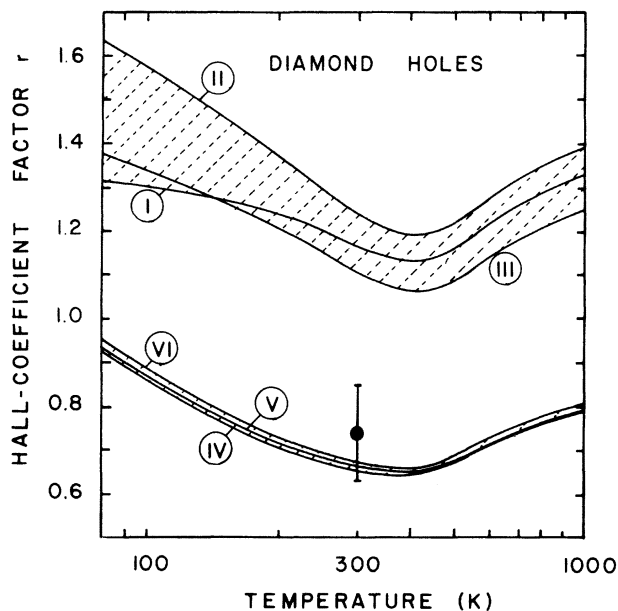


FIG. 1. Hall-coefficient factor as a function of temperature for the case of lattice scattering only. Different curves refer to calculations performed with different sets of inverse valence-band parameters as given in Table I. Solid point refers to experimental value. Shaded region evidences analogies of behavior of two groups of sets (see text).

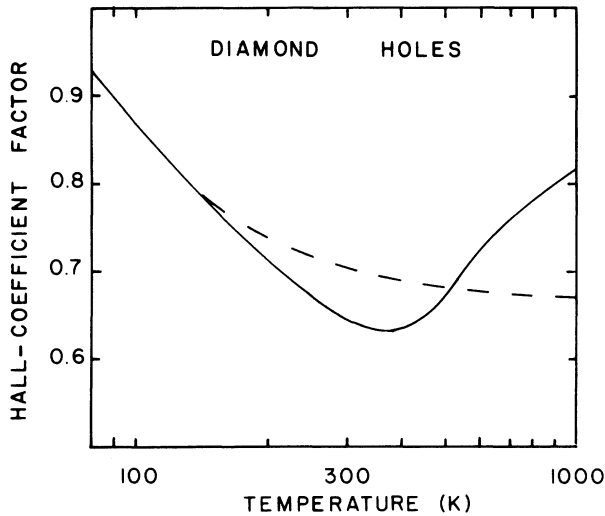


FIG. 2. Theoretical calculations of the Hall-coefficient factor performed with set V and no ionized impurity scattering. Dashed curve refers to the case when only acoustic scattering is considered.

300 K and, in general, the value of  $r$  is found to be lower when impurity scattering is considered than for the pure lattice case. In particular, owing to the difference in the response of drift and Hall mobilities to changes in impurity concentration, at the lowest temperatures  $r$  is found to have a minimum for  $N_I \approx 10^{14} \text{ cm}^{-3}$ ; furthermore, for values of  $N_I$  between about  $10^{12}$  and  $10^{15} \text{ cm}^{-3}$  calculations lead us to expect an approximately constant region of  $r$  below about 300 K.

The experimental Hall-coefficient factor  $r$  has been calculated from the ratio between Hall and drift mobility data. Drift mobility in the range of temperatures  $100 < T < 1000 \text{ K}$  has been extrapolated from results obtained with the time-of-flight technique<sup>19</sup> on high-purity diamond sample (acceptor impurity concentration  $N_A \equiv 10^{12} - 10^{13} \text{ cm}^{-3}$ ).

Hall mobility as function of temperature has been taken from measurements of the Hall effect undertaken during photoexcitation on samples with analogous high-purity characteristics<sup>21</sup> and from standard Hall measurements on samples with donor concentration  $N_D = 5.6 \times 10^{15} \text{ cm}^{-3}$  and  $N_A = 3.2 \times 10^{16} \text{ cm}^{-3}$ .<sup>22</sup>

In the common range of temperature different Hall-coefficient data have been found to be in agreement within experimental uncertainty, which is estimated to be  $\pm 15\%$ , thus supporting the reliability of the values of  $r$  reported here (see Fig. 4).

A full comparison between theory and experiment is given in Fig. 4. Below about 300 K the agreement is within the experimental uncertainty. Above 300 K the theoretical curve lays systematically below the

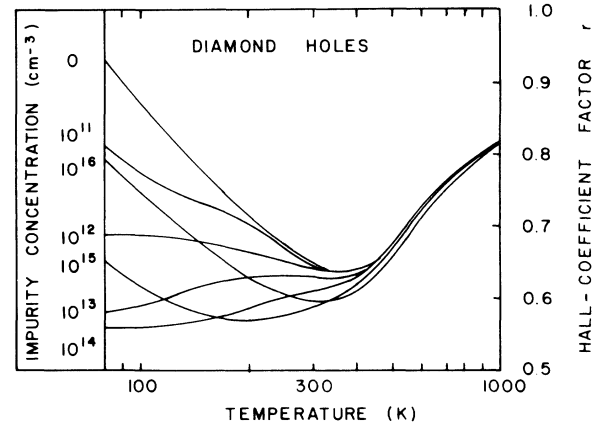


FIG. 3. Theoretical calculations of the Hall-coefficient factor (right scale) performed with set V for the given impurity concentrations (values on the left give the impurity concentration of the associated curve).

experimental points. The main reason for this high-temperature discrepancy is the neglect of the split-off band. The warping of the split-off band is similar to that of the light-hole band. Therefore, the Hall-coefficient factors for the two bands should be similar. As a result including the split-off band in the calculations should increase the value of the Hall-coefficient factor by 10–15% in the range above room temperature. Thus even considering that the theoretical treatment of impurity scattering is still a debated problem,<sup>23</sup> the reasonable agreement found above 300 K, where impurity scattering is negligible, further supports present findings.

In summary, owing to the lack of any adjustable parameters between theory and experiment, the overall agreement should be considered satisfactory

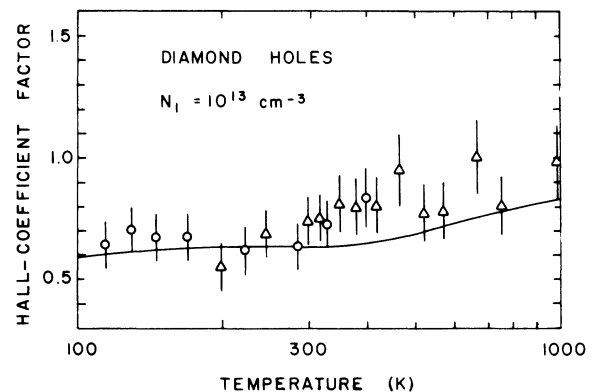


FIG. 4. Comparison between theoretical and experimental Hall-coefficient factor. Theory uses set V and includes ionized impurity scattering with concentration  $N_I = 10^{13} \text{ cm}^{-3}$ .  $\circ$  and  $\Delta$  refer to data obtained from Hall-mobility measurements of Refs. 21 and 22, respectively (see text).

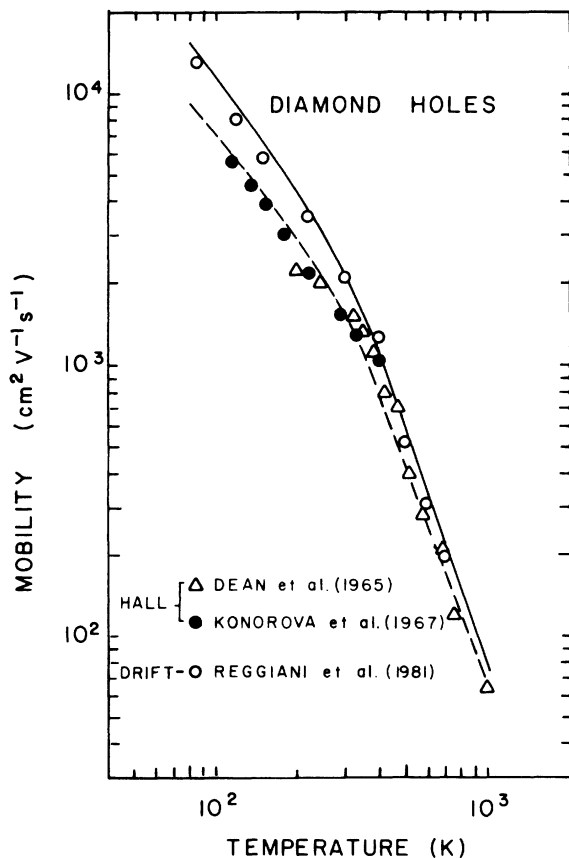


FIG. 5. Mobility as a function of temperature. Solid and dashed curves refer to drift and Hall mobility calculated as in Fig. 4.  $\circ$  refers to drift-mobility data of Ref. 19;  $\bullet$  and  $\triangle$  refer to Hall-mobility data of Refs. 21 and 22, respectively.

and taken as a valuable test to prove the better reliability of the valence-band parameters of sets IV, V, and VI as compared to sets I, II, and III. For completeness, Fig. 5 reports the results of the drift and

Hall mobility as a function of temperature obtained as best fit of experiments with set V. It is worth noting that from present calculations the values of acoustic and optical deformation-potential parameters are found to be slightly higher (about 35%) than the values of Ref. 8.

#### IV. CONCLUSIONS

This paper reports an analysis of the Hall-coefficient factor  $r$  for holes in natural diamond. In strict analogy with the similar case of Si, experiments give evidence for values of  $r$  less than unity in the whole temperature range here investigated  $100 < T < 1000$  K. A microscopic interpretation correlates this result with the warped and nonparabolic features of the valence band. Fit between theory and experiment is shown to be a selective test for the different sets of the inverse valence-band parameters available from literature. Results prove that the sets IV, V, and VI (see Table I), which lead to a more pronounced anisotropic character of the band, are the most reliable; in addition, when high-field drift velocity modeling is taken as a further test, set V (i.e.,  $|A| = 3.61$ ,  $|B| = 0.18$ , and  $|C| = 3.67$ ) emerges as the preferred one.

#### ACKNOWLEDGMENTS

The authors wish to thank Dr. E. A. Konorova for having brought the problem to their attention and Dr. A. Baldereschi for having provided valuable information on the valence-band structure of diamond. The Computer Centre of the Modena University is acknowledged for having provided part of the computer facilities. Two of us (D. W. and S. Z.) wish to acknowledge the support of the National Sciences and Engineering Research Council of Canada.

<sup>1</sup>G. Gagliani and L. Reggiani, *Nuovo Cimento B* **30**, 207 (1975).

<sup>2</sup>G. G. Hall, *Philos. Magazine* **3**, 429 (1958).

<sup>3</sup>C. J. Rauch, *Phys. Rev. Lett.* **7**, 83 (1961); *Proceedings of the Sixth International Conference on the Physics of Semiconductors, Exeter, 1962* (IOP, London, 1962), p. 276.

<sup>4</sup>P. Lawaetz, *Phys. Rev. B* **4**, 3460 (1971); in this paper the  $\gamma_2$  value of Table II should be corrected in  $\gamma_2 = 0.42$ , thus there is no sign difference between  $\gamma_2$  and  $\gamma_3$  and the formalism cited is valid; P. Lawaetz (private communication).

<sup>5</sup>W. Saslow, T. K. Bergstresser, and M. L. Cohen, *Phys. Rev. Lett.* **16**, 354 (1966); A. Baldereschi (private communication).

communication).

<sup>6</sup>W. van Haeringen and H. G. Junginger, *Solid State Commun.* **7**, 1135 (1969); A. Baldereschi (private communication).

<sup>7</sup>J. A. van Vechen, *Bull. Am. Phys. Soc.* **237** (1972); A. Baldereschi (private communication).

<sup>8</sup>L. Reggiani, *J. Phys. Soc. Jpn.* **49**, 317 (1980).

<sup>9</sup>H. Nakagawa and S. Zukotynski, *Can. J. Phys.* **56**, 364 (1978).

<sup>10</sup>J. F. Lin, S. S. Li, L. C. Linares, and K. W. Teng, *Solid State Electron.* **24**, 827 (1981).

<sup>11</sup>E. G. S. Paige, *The Electrical Conductivity of Germanium*, edited by A. F. Gibson and R. E. Burgess (Heywood, London, 1964), p. 15ff.

- <sup>12</sup>E. O. Kane, *J. Phys. Chem. Solids* **1**, 82 (1956).
- <sup>13</sup>K. Takeda, K. Sakui, and M. Sakata, *J. Phys. C* **15**, 767 (1982).
- <sup>14</sup>F. Szmulowicz and F. L. Madarasz (private communication).
- <sup>15</sup>H. Nagakawa and S. Zukotynski, *Can. J. Phys.* **55**, 1485 (1977).
- <sup>16</sup>G. L. Bir and G. E. Pikus, *Fiz. Tverd. Tela Leningrad* **2**, 2287 (1960) [*Sov. Phys.—Solid State* **2**, 2039 (1961)].
- <sup>17</sup>M. Tiersten, *IBM J. Res. Dev.* **5**, 122 (1961); *J. Phys. Chem. Solids* **25**, 1151 (1961).
- <sup>18</sup>M. Costato and L. Reggiani, *Phys. Status Solidi B* **58**, 461 (1973).
- <sup>19</sup>L. Reggiani, S. Bosi, C. Canali, F. Nava, and S. F. Kozlov, *Phys. Rev. B* **23**, 3050 (1981).
- <sup>20</sup>P. Lawaetz, *Phys. Rev.* **174**, 867 (1968).
- <sup>21</sup>E. A. Konorova and S. Shevchenko, *Fiz. Tekh. Poluprovodn.* **1**, 364 (1967) [*Sov. Phys.—Semicond.* **1**, 299 (1967)].
- <sup>22</sup>P. J. Dean, E. C. Lightowers, and D. R. Wight, *Phys. Rev.* **140**, A352 (1965).
- <sup>23</sup>D. Chattopadhyay and H. J. Queisser, *Rev. Mod. Phys.* **53**, 745 (1981).